

Digital surface shadow for fly-cut surfaces utilizing dynamic axis data

Sabrina Stemmer¹, Lars Schönemann^{1,2}, Oltmann Riemer¹, Bernhard Karpuschewski^{1,2}

¹Leibniz Institut für Werkstofforientierte Technologien IWT, Laboratory for Precision Machining LFM, Badgasteiner Straße 2, 28359 Bremen, Germany

²MAPEX Center for Materials and Processes, University of Bremen, Germany

stemmers@uni-bremen.de

Abstract

The digitalization of manufacturing processes enables the tracing of dynamic influences in the production processes to specific characteristics of the final product. In this case, existing models for surface simulation of ultra-precision fly-cut surfaces were extended to dynamically incorporate acquired axis data of the machine tool to further improve the prediction of the machined surface topography. Therefore, a signal splitter was incorporated into the machine tool's control systems, which allows for a seamless readout of the axes' encoder signals without influencing the control system of the machine itself. The readout of the sensors was referenced to the machine tool and workpiece coordinate system and then fed into the dynamic model, which periodically examines the interaction of tool and workpiece (i.e. the cutting procedure) and calculates the resulting surface geometry, i.e. topography and form.

The topic to be presented is a detailed description of the applied modeling and simulation framework, the integration of the axis data as well as a validation of this approach, which is illustrated by three examples. While the surface roughness comparison showed clear differences, certain characteristics could be found in the corresponding image when comparing the simulated surface features with the actual generated topography.

Precision machining, surface shadow, simulation

1. Introduction

Digitalization has been gaining importance in manufacturing technology for decades and it has become an integral part of modern production environments. Production data and integrated machine data interfaces can be used for a wide variety of purposes, such as process control, maintenance and interruption planning or to make statements about production progress or component quality. The last point in particular is important for precision machining.

Today ultra-precision parts are applied in a widespread field of sectors such as the automotive, fusion, metrology and aerospace industries, in the health sector and in the field of photography to afford very different functions. Therefore the range of parts is diverse and extends from optical components such as flat, pyramidal, spherical and aspherical-mirrors, ellipsoids, toroids, optics, microlenses, spectrometers installed inside satellites, components for vehicle lighting systems, energy conductors e.g. waveguides, air bearing components, lenses for photography and laser applications to ultra-precision tools like mould inserts.

Ultra-precision manufacturing is a time consuming and challenging task, because of the tiny scaled chip removal and the fact that most steps in this process are nearly invisible to the human eye. This leads to the process requiring long machine production times and to a high uncertainty about the quality of the workpiece along the whole process.

In order to make an adequate prediction of the result at the end of the machining process, a simulation of the generated surface is built from axis data of the manufacturing machine. Ideally, the waste of energy, resources, time and costs can be avoided by recognizing critical moments in the production process at an early stage during runtime and taking appropriate

countermeasures. The development of this approach is pursued with the help of a digital surface shadow in an ultra-precision fly-cutting process.

1.1. Previous work

In recent decades numerous research projects have been carried out to optimize ultra-precision fly-cutting processes. Several approaches aim the high speed cutting of ultra-precise surfaces in order to reduce the production time [1, 2]. Other approaches investigate the vibration [3] and the prevention of critical machine states or the identification of critical events [4, 5]. Fewer approaches explore the live representation of the surface. A foundation to build up a digital surface twin for fly-cutting processes was laid by the authors in 2022 [6]. Two different models, a numerical height map and a dixel-based simulation model for generating the surface were developed. The incorporation of axis data took place after the machining process. For the dixel approach the surface is split up in dixel and intersection points. The tool engagement is determined as sweep-volume and for the simulation the position data is transformed to a path of the tool-center-point.

For the height map approach the complete surface is tessellated into smaller patches containing height points. The tool engagement apex points, referring to the height, are determined using the process parameters such as feed, raster spacing and fly-cutting radius. To handle overlapping and the failure addition of material the minimum of either the tool footprint or of the existing surface is saved in the height map. Both approaches achieved high accuracy in predicting the surface.

In the presented work the height map approach is extended in order to set up a data interface for axis data, a live data handling and a parallel simulation of the surface while the machine is running.

1.2. Intention

The intention of the presented work is a simulation of the surface, parallel to the machining process utilizing live axis data and static process data. This approach is validated in machine tests and the results of the simulation is compared to the physical surface measured by white light interferometry. Section 2 presents the methodology, describing first in 2.1 the experimental setup and the materials utilized for this purpose. Then in 2.2 the data operations are briefly outlined followed by 2.3 explaining the simulation. Section 3 presents the results of the simulation divided into the presentation of the simulated surface in 3.1 and the measured surface in 3.2. Followed by the comparison of simulated and measured surfaces presented in 3.3 and a disturbance test described in 3.4. Finally, section 4 summarizes the contents.

2. Methodology

The methodology for setting up the surface simulation essentially consists of two main parts: The management of live data and the visualization of the surface. The dynamic axis data is obtained within a fly-cutting process that is depicted in Figure 1.

2.1 Experimental setup and materials

The utilized ultra-precision 5-axis machine tool Nanotech 350 FG is placed in the Laboratory for Precision Machining LFM in Bremen on a marble base in an air-conditioned room in order to eliminate external influences. The material of the workpiece, German silver, which is a Nickel alloy with copper and zinc, was also chosen for this reason. The surface is generated in a fly-cutting process with a fly-cut radius $r_{fly} = 67 \text{ mm}$ using monocrystalline diamond as cutting material with a tool nose radius $r_{\epsilon} = 0.762 \text{ mm}$.

To achieve the axis data during the machine run an interface system EIB 741 (Heidenhain) is used, which splits the axis signal directly from the machine control cabinet into two signals; one for the machine control and one for the laptop input socket. Furthermore a Talysurf CCI HD (Taylor Hobson) while light interferometer is utilized to measure the generated surfaces after machining.

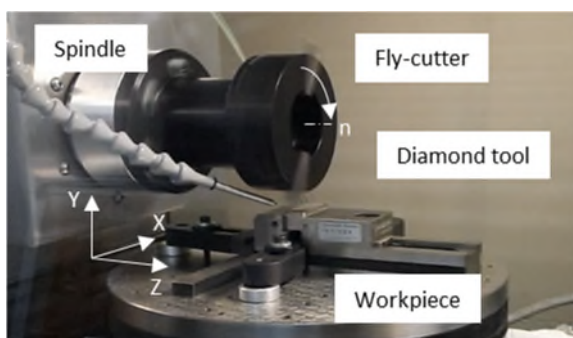


Figure 1. Surface machining of a workpiece with a diamond tool mounted in a fly-cutter on the main spindle

2.2 Axis Data

The data of the machine axis are routed to a software interface where the arranged data packets are streamed into a file. This is done by the signal splitter before the computation job of the machine itself. After that a Python script reads the latest data out of the file and converts the values from the raw format to the actual length scale.

2.3 Simulation

When the simulation starts the current position is saved as reference position and the first tool operation is visible. If the

axis data changes, the surface is updated simultaneously. The simulated tool sweep is repositioned periodically as the tool is moved relative to the workpiece.

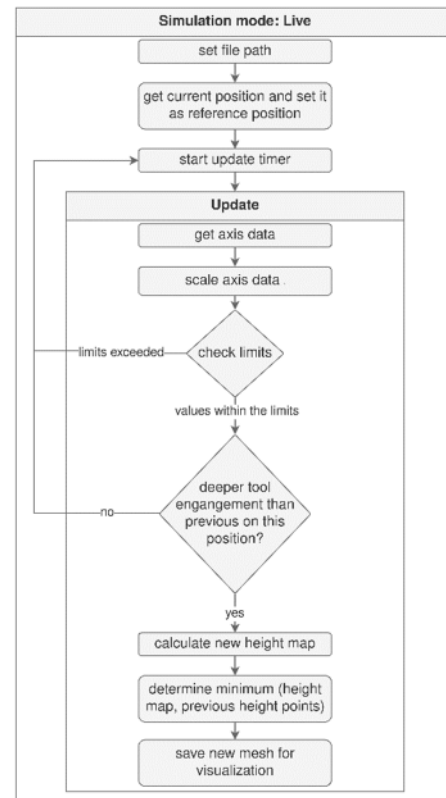


Figure 2. Program flowchart of the live simulation

If the new height is deeper than the current height of this tool position, the mesh is changed and passed to the visualization in order to show the new surface. The calculation of the height points is mainly dependent on the radius of the diamond tool and the fly-cut radius, but also on the feed and the raster space, since they define the tool engagement. An outlined program flowchart is shown in Figure 2.

Although there is a data transition in both processes, the update function of the new height map and the visualization function, can operate independently of each other. While the process is running it is possible to move and zoom the visualization to check the generated surface and stop the machining process when a critical fault is identified. The prerequisite is a suitable choice of the resolution parameter to prevent long calculation times. With the developed graphical user interface a visualization and several options e.g. to save the current mesh and a picture or to edit the reference positions are presented, as shown in Figure 3.

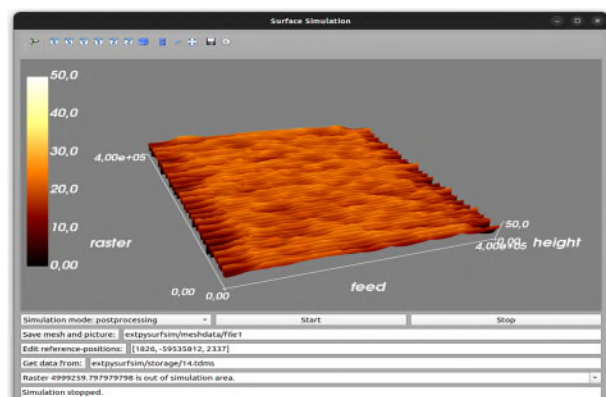


Figure 3. Graphical user interface of the simulation

3. Results

In order to be able to find the section for the measurement, the tool was moved close to the simulation area during tool engagement. This resulted in features at the left and right edge of the section. During machining the simulated surface is visualized and shows these features. In addition the simulation input axis data and the resulting surface could be saved during the machining session.

As the tool path data is handled separately from the visualization, the resulting surface geometry can be repeatedly generated in the post processing mode. This reveals the advantage of a higher resolution and the opportunity to change simulation parameters e.g. the smoothing value.

3.1. Simulated surface

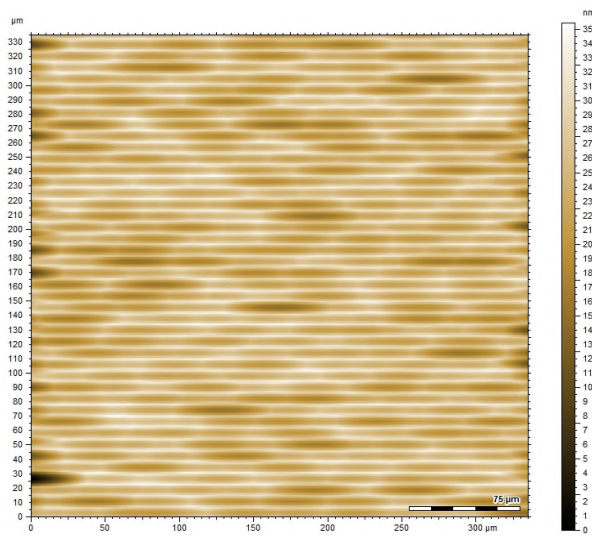


Figure 4. Simulated Surface as a result after the process (sample 5)

The post processed simulated surface from the machine test setup of the presented example is depicted in Figure 4. Conspicuous are the features on the edge; some are more pronounced e.g. the feature near the bottom left corner. The features in the middle are less noticeable.

3.2. Measured surface

Figure 5 shows the measured surface referring to the simulated surface depicted in Figure 4.

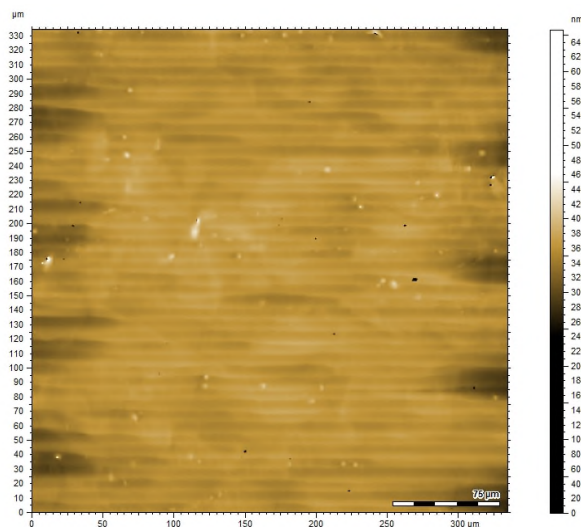


Figure 5. Measurement of the surface (sample 5)

In the measured surface the edge features are also clearly visible, although in a slightly different way. In comparison it looks as if the simulated image has been sharpened. This could be due to the different height scaling. The measured image is displayed on a scale ranging from approx. 250 to approx. 400 nm, with a maximum range of 650 nm. On the other hand, the simulated image is displayed on a scale ranging from zero to approx. 35 nm, utilizing the full range of the scale, although this is dependent on the simulation, the zoom and the scale settings.

3.3. Feature and roughness comparison

In Figure 6 three distinctive features are selected for comparison.

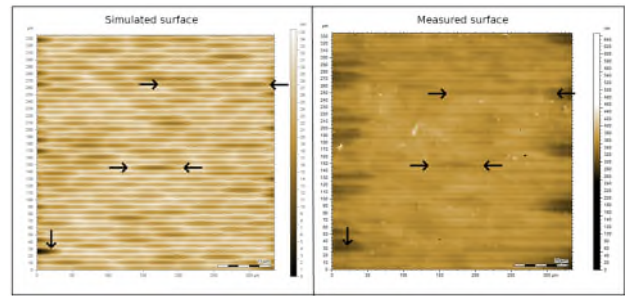


Figure 6. Comparison of the features in the simulated surface and the measurement of the first example (sample 5)

Although there were some matching features, the result is not entirely clear, as not all features were found in the respective comparison image.

The second example presented here also shows ambiguous results, according to Figure 7.

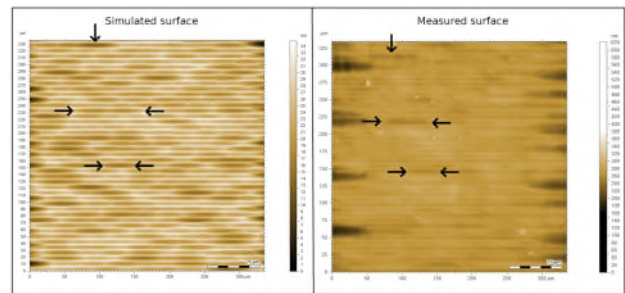


Figure 7. Comparison of the features in the simulated surface and the measurement of the second example (sample 12)

For this reason the roughness values of the surfaces were compared, see Table 1. The comparison shows for the mean arithmetic height clear differences of $\Delta Sa = 6.6 \text{ nm}$ between the parallel simulated and the measured surface and for the maximum height $\Delta Sz = 601.75 \text{ nm}$. The differences between the post processed simulated and the measured surface vary in the same area. In percentage terms, the Sa values of the simulated surfaces are approx. ten times higher.

Table 1. Comparison of the surface parameters

Surface roughness of the second example (sample 12), ISO 25178			
[nm]	Parallel simulated surface	Post processed surface (higher resolution, generation not in real-time)	Measured surface
Sa	2.18	3.12	8.78
Sz	19.85	34.80	621.60

One reason for the differences may be the mechanism of the simulation, which causes a limitation of height outlier values. This can be seen even more clearly in the disturbance test presented below.

3.4. Disturbance test

The post processed simulated surface of the machine test with introduced disturbances is investigated in the following part.

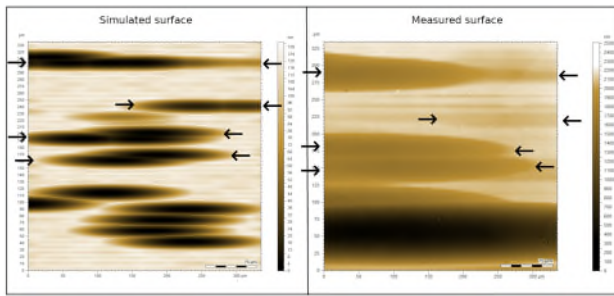


Figure 8. Comparison of the features in the simulated surface and the measurement of the third example (sample 9)

Figure 8 shows the external influences clearly in both the simulated and the measured image. Although the same sharp effects can be observed as in the previous presented samples, a connection of the simulated image with the measured one can be determined.

The surface roughness parameters in Table 2, however show a discouraging result, that does not reflect the real situation. Although the values are higher than for the samples without interference, with differences of $\Delta Sa = 419.28 \text{ nm}$ between the parallel simulated and the measured surface and $\Delta Sz = 2462.19 \text{ nm}$, they are still far from the values of the measured surface. The Sa values of the simulated surfaces also differ greatly in percentage terms. It should be noted that even the smallest outliers, that occur e.g. due to the material, influence the measurement of the maximum height.

Table 2. Comparison of the surface parameters

Surface roughness of the third example (sample 9), ISO 25178			
[nm]	Parallel simulated surface	Post processed surface (higher resolution, generation not in real-time)	Measured surface
Sa	2.72	35.46	422.00
Sz	44.81	130.70	2507.00

4. Conclusion

To summarize, a live axis data stream was implemented and fed into a simulation of the generated surface during the machining process.

The experimental setup and the materials as well as the data operations and the simulation were described. As a result of the simulation the visualization was compared with the measured surface in a qualitative and quantitative way. With a disturbance test the observations could be confirmed.

In conclusion the axis data seem to be a good choice for this purpose, but the evaluation did not reveal a clear result. While a similarity cannot be denied in the image comparison a direct coincidence cannot be ruled out. The surface roughness comparison in particular showed very clear differences. Thus further work in the area of limit data management and resolution improvement is necessary. This work represents preliminary work that can be expanded and utilized for optimizing fly-cutting processes.

References

- [1] Brinksmeier E and Schönemann L 2022 Ultra-precision High Performance Cutting: Report of DFG Research Unit FOR 1845 1 10.1007/978-3-030-83765-5
- [2] Schönemann L et al. 2020 Synergistic approaches to ultra-precision high performance cutting J. CIRP Journal of Manufacturing Science and Technology 28 p. 38-51 10.1016/j.cirpj.2019.12.001
- [3] Ding Y, Rui X, Chen Y, Lu H, Chang Y and Wei W 2022 Theoretical and experimental investigation on the surface stripes formation in ultra-precision fly cutting machining J. The International Journal of Advanced Manufacturing Technology 124 p. 1041-1063 10.1007/s00170-022-10493-9
- [4] Wu L, Sha K, Tao Y, Ju B and Chen Y 2023 A Hybrid Deep Learning Model as the Digital Twin of Ultra-Precision Diamond Cutting for In-Process Prediction of Cutting-Tool Wear J. Appl. Science 13 p.6675 10.3390/app13116675
- [5] Selvaraj V, Xu Z and Min S 2022 Intelligent Operation Monitoring of an Ultra-Precision CNC Machine Tool Using Energy Data J. International Journal of Precision Engineering and Manufacturing-Green Technology 10 10.1007/s40684-022-00449-5
- [6] Schönemann L, Riemer O, Karpuschewski B, Schreiber P, Klemme H and Denkena B 2022 Digital surface twin for ultra-precision high performance cutting J. Precision Engineering. 77 p. 349-359 10.1016/j.precisioneng.2022.06.010